

Surprising toxicity and assembly behavior of amyloid β -protein oxidized to sulfone

Panchanan Maiti*, Roberto Piacentini§, Cristian Ripoli§, Claudio Grassi§, and Gal Bitan*,†,‡

*Department of Neurology, David Geffen School of Medicine, †Brain Research Institute, and ‡Molecular Biology Institute, University of California at Los Angeles, 635 Charles E. Young Drive South, Los Angeles, CA 90025, USA. §Institute of Human Physiology, Catholic University Medical School, Largo F. Vito 1, Rome 00168, Italy.

Corresponding author: Gal Bitan, Ph.D., Department of Neurology, Neuroscience Research Building 1, Room 451, Charles E. Young Drive South, Los Angeles, CA 90095, USA. Tel: 1-310-206-2082, Fax: 1-310-206-1700; E-mail: gbitan@mednet.ucla.edu

Running title: Toxicity and assembly of A β -sulfone

Synopsis

Amyloid β -protein ($A\beta^1$) is believed to cause Alzheimer's disease (AD). $A\beta_{42}$ is substantially more neurotoxic than $A\beta_{40}$ and this increased toxicity correlates with existence of unique $A\beta_{42}$ oligomers. Met^{35} oxidation to sulfoxide or sulfone eliminates the differences in early oligomerization between $A\beta_{40}$ and $A\beta_{42}$. Met^{35} oxidation to sulfoxide was reported to decrease $A\beta$ assembly kinetics and neurotoxicity whereas oxidation to sulfone rarely has been studied. Based on these data, we expected that oxidation of $A\beta$ to sulfone also would decrease its toxicity and assembly kinetics. To test this hypothesis, we compared systematically the effect of the wild-type, sulfoxide, and sulfone forms of $A\beta_{40}$ and $A\beta_{42}$ on neuronal viability, dendritic spine morphology, and macroscopic Ca^{2+} currents in primary neurons, and correlated the data with assembly kinetics. Surprisingly, we found that in contrast to $A\beta$ -sulfoxide, $A\beta$ -sulfone was as toxic, and aggregated as fast, as WT $A\beta$. Thus, although $A\beta$ -sulfone is similar to $A\beta$ -sulfoxide in its dipole moment and oligomer size distribution, it behaves similarly to WT $A\beta$ in its aggregation kinetics and neurotoxicity. These surprising data decouple the toxicity of oxidized $A\beta$ from its initial oligomerization and suggest that our current understanding of the effect of Met oxidation in $A\beta$ is limited.

Keywords: Alzheimer's disease, amyloid β -protein, methionine, oxidation, oligomer

Introduction

Alzheimer's disease (AD) is characterized by memory loss and progressive cognitive decline [1]. Extracellular amyloid plaques comprising predominantly fibrillar amyloid β -protein ($A\beta$) and intracellular neurofibrillary tangles made of hyperphosphorylated tau are neuropathological hallmarks of AD [2]. Abundant evidence suggests that assembly of $A\beta$ into pre-fibrillar, neurotoxic oligomers initiates the disease process in AD and formation of amyloid plaques and neurofibrillary tangles follow neuronal injury by $A\beta$ oligomers [3].

$A\beta$ exists predominantly in two major forms comprising 40 ($A\beta_{40}$) or 42 ($A\beta_{42}$) amino acid residues. Genetic, physiologic, and biochemical evidence indicates that $A\beta_{42}$ plays a predominant role in the pathogenesis of AD [4] although it is ~ 10 -times less abundant than $A\beta_{40}$ [5]. In the AD brain, $A\beta_{42}$ is the main component of parenchymal plaques whereas $A\beta_{40}$ is the main component of vascular deposits [6]. $A\beta_{42}$ aggregates faster and is substantially more neurotoxic than $A\beta_{40}$ [7].

Study of $A\beta$ oligomerization *in vitro* using photo-induced cross-linking of unmodified proteins (PICUP) and ion-mobility-mass-spectrometry has revealed that the oligomer size distributions of $A\beta_{40}$ and $A\beta_{42}$ are distinct [8, 9]. $A\beta_{40}$ exists mainly as a mixture of monomer, dimer, trimer and tetramer, whereas $A\beta_{42}$ preferentially forms pentamer and hexamer units, termed paranuclei, which self-associate into higher order oligomers [8, 9]. The distinct oligomerization patterns of $A\beta_{40}$ and $A\beta_{42}$ correlate with the difference in the toxicity of the two $A\beta$ alloforms and may explain these differences. This suggests that the C-terminal region of $A\beta$ is a crucial factor in $A\beta$ assembly and toxicity. Supporting this hypothesis, structural studies using experimental and computational methods have identified substantial differences in the flexibility and conformational preferences of the C-terminal region of $A\beta_{40}$ and $A\beta_{42}$ [10-12].

The single Met residue in $A\beta$, Met^{35} , is located in the middle of the hydrophobic C-terminal region of

¹ **Abbreviations:** AD, Alzheimer's disease; $A\beta$, amyloid β -protein; ANOVA, analysis of variance; DMEM, Dulbecco's Modified Eagle's Medium; EM, electron microscopy; FMOC, 9-fluorenylmethoxycarbonyl; HFIP, 1,1,1,3,3,3-hexafluoroisopropanol; LDH, lactate dehydrogenase; MTT, 3-(4,5-dimethylthiazol-2-yl)-2,5-diphenyltetrazolium bromide; OD, Optical density; PICUP, photo-induced cross-linking of unmodified proteins; ROS, reactive oxygen species; TUNEL, terminal deoxynucleotidyl transferase dUTP nick end labeling.

A β and is readily oxidized *in vivo* [13]. The dramatic increase in the polarity of the Met side chain that occurs upon oxidation (Table 1) has a profound effect on the hydrophathy of the entire region [14]. A β in which Met³⁵ is oxidized to sulfoxide (A β -sulfoxide) has been found in amyloid plaques of AD brain [13] and consequently has been the subject of many studies [15]. Despite the abundance of literature on the subject, is not clear whether A β -sulfoxide contributes to AD etiology or results from the highly oxidative environment around amyloid plaques where fibrillar A β may be trapped for long periods and get oxidized.

In addition to oxidation to sulfoxide, Met can undergo a second oxidation reaction yielding Met-sulfone (Table 1). This reaction is less common than oxidation of Met to Met-sulfoxide *in vivo*, yet Met-sulfone has been observed in the brain of patients with AD or Parkinson's disease [16] in the anti-oxidant protein DJ-1. Ali et al. have proposed that A β -sulfone also might form *in vivo* and was not observed so far simply because it was not looked for [17].

Oxidation of Met³⁵ to sulfoxide has been reported to decrease formation of A β 40 trimers and tetramers [18], lower A β assembly kinetics [11, 19], and reduce A β neurotoxicity [15, 20]. Solution-state NMR studies have shown that the lower assembly kinetics and toxicity correlated with higher conformational flexibility in the C-terminal region of A β -sulfoxide relative to wild-type (WT) A β [19]. The assembly kinetics and toxicity of A β -sulfone have not been reported previously.

A PICUP study of the effect of Met³⁵ oxidation in A β revealed striking differences between A β 40 and A β 42 [14]. The oligomer size distribution of A β 40 was unaffected by oxidation of Met³⁵. In contrast, oxidation of Met³⁵ in A β 42 to either sulfoxide or sulfone was found to abolish paranucleus formation and produce oligomer size distributions indistinguishable from those of A β 40 [14]. In agreement with these observations, molecular dynamics simulations of the WT, sulfoxide, and sulfone forms of A β 42 monomers showed that the two oxidized forms adopted conformations that were distinct from that of WT A β 42, both in secondary structure and in global fold [21]. In particular, long-range interactions between the C-terminal region and the central hydrophobic cluster (CHC), which were prominent in WT A β 42, and have been observed in other modeling studies of A β 42 monomers [22] and oligomers [10, 23], were absent in the simulations of the two oxidized forms [21]. Rather, the sulfoxide and sulfone groups, which are hydrogen-bond acceptors, formed hydrogen bonds with backbone amide groups in the C-terminal regions stabilizing short-range turn conformations. In modeling studies comparing A β 40 and A β 42 oligomerization [10, 23] the interaction between the C-terminus and the CHC regions was substantially less prominent in A β 40 compared to A β 42, suggesting that this structure may be necessary for paranucleus formation.

Attempting to correlate the structural and functional data, we hypothesized that the A β oligomer size distributions observed using PICUP correlated with toxicity. If this hypothesis were correct, oxidation of A β 40 would be predicted to have little effect on toxicity, whereas oxidation of A β 42 to sulfoxide or sulfone would result in toxicity lower than that of WT A β 42 and similar to A β 40. The lower toxicity of A β 42-sulfoxide reported in the literature [15, 20, 24] supported this hypothesis, yet we found a dearth of information regarding the effect of oxidation of Met to Met-sulfoxide in A β 40 or oxidation of either A β alloforms to sulfone.

Because Met-sulfoxide can be reduced to Met *in vivo* by methionine-sulfoxide reductases [25], when cells are treated with A β -sulfoxide, they also are treated with unoxidized A β . The ratio of A β -sulfoxide to WT A β depends on the kinetics of Met-sulfoxide reduction relative to peptide degradation. Additional factors determining the observed toxicity are the assembly state of each A β form in the context of the cellular environment [26] and the mechanisms by which each form causes toxicity, all of which are poorly understood. Because Met-sulfone is not reduced *in vivo* [27], studying the effect of A β -sulfone on cultured neurons is a "clean" system compared to A β -sulfoxide. Thus, to test our hypothesis of the effect of Met oxidation on A β assembly and toxicity, we compared the WT, sulfoxide, and sulfone forms of A β 40 and A β 42 using assays that measure assembly kinetics, cell viability, and cellular function in primary cortical or hippocampal neurons. Surprisingly, we found that contrary to our

prediction, A β -sulfone behaved similarly to unoxidized A β and distinctly from A β -sulfoxide, raising new questions regarding the mechanisms by which each A β form causes toxicity.

Experimental

Peptides synthesis- A β 40, [Met(O)³⁵]A β 40, [Met(O₂)³⁵]A β 40, A β 42, [Met(O)³⁵]A β 42, and [Met(O₂)³⁵]A β 42 were synthesized by incorporating Fmoc-Met(O) or Fmoc-Met(O₂) (EMD Biosciences, San Diego, CA) in position 35 where appropriate, purified, and characterized in the UCLA Biopolymers Laboratory. Quantitative amino acid analysis and mass spectrometry were used to characterize the expected compositions and molecular weights, respectively, for each peptide.

Preparation of peptide solutions- Purified peptides were stored as lyophilized powders at -20°C. Before use, peptides were treated with 1,1,1,3,3,3-hexafluoroisopropanol (HFIP, TCI America, Portland, OR) to disassemble pre-formed aggregates and stored as dry films at -20°C as described previously [28]. Immediately before use, films were dissolved in 60 mM NaOH at 10% of the desired volume. For biophysical measurements, the solution then was diluted to 50% of the desired volume with deionized water (18.2 M Ω produced by a Milli-Q system, Millipore, Bedford, MA) and sonicated for 1 min. Then, the solution was diluted with 20 mM sodium phosphate, pH 7.4, to 10 μ M. The pH was adjusted, if necessary, with H₃PO₄ or 1M NaOH. Alternatively, peptides were prepared by dilution into cell culture media, similar to the preparation for toxicity experiments. For toxicity experiments, peptides were diluted with cell-culture media after initial dissolution in 10% NaOH, and then sonicated for 1 min. Then, the peptides were diluted in culture media to the final concentration, which was 10 μ M unless otherwise stated.

Animals- Experiments performed in UCLA were compliant with the National Research Council Guide for the Care and Use of Laboratory Animals and were approved by the UCLA Animal Research Council and the Ethics Committee. Experiments performed in the Catholic University of Rome complied with Italian Ministry of Health guidelines, with national laws (Legislative decree 116/1992), and with European Union guidelines on animal research (No. 86/609/EEC). For experiments in UCLA, pregnant (E18) Sprague-Dawley rats were purchased from Charles River Laboratory (Wilmington, MA). In the Catholic University, Sprague-Dawley rats were bred in-house.

Cell culture- For TUNEL assay and dendritic spine morphology experiments, primary cortical or hippocampal neurons, respectively, were prepared as described previously by Segal and Manor [29]. Briefly, E18 pregnant rats were euthanized with CO₂ and the pups were collected immediately. The brains were dissected in chilled Leibovitz's L-15 medium (ATCC, Manassas, VA) in the presence of 1 μ g/ml penicillin/streptomycin (Invitrogen, Carlsbad, CA). The tissue was incubated with 0.25% trypsin-EDTA (ATCC) for 30 min and then mechanically dissociated in a small volume of Leibovitz's L-15 medium using a fire-polished Pasteur pipette. Cortical neurons were used for cell viability assays. They were suspended in Dulbecco Modified Eagle's Medium (DMEM, obtained from ATCC) containing 10% heat-inactivated fetal bovine serum (ATCC) and penicillin/streptomycin (1 μ g/ml) and plated in poly D-lysine (0.1 mg %, Sigma)-coated coverslips (Fisher Scientific, Tustin, CA) at a density of 3 \times 10⁵ cells/ml. Hippocampal neurons were used for dendritic spine studies. They were suspended in neurobasal media (GIBCO, Carlsbad, CA) containing B27 growth factor and 20 mM glutamine and plated on poly D-lysine (0.1 mg%, Sigma) cover slips. The cultures were maintained at 37°C in a humidified atmosphere of 5% CO₂ for 6 d for cell viability experiments and for 21 d for dendritic spines experiments. Twenty-four hours after plating, the medium was replaced with fresh DMEM/neurobasal media supplemented with 5 μ M cytosine β -D-arabinofuranoside (Sigma) to inhibit the proliferation of glial cells.

For measurements of Ca²⁺ currents, primary cortical neurons were obtained from E17–E19 rat embryos as described previously by Dravid et al. [30] with minor modifications. Briefly, cortices were dissected and incubated for 10 min at 37°C in phosphate-buffered saline (PBS) containing trypsin-EDTA (0.025%/0.01% w/v, Biochrom AG, Berlin, Germany). The tissue then was mechanically dissociated at room temperature using a fire-polished Pasteur pipette and the cell suspension was harvested and

centrifuged at 1,100 rpm for 8 min. The pellet was suspended in 88.8% Minimum Essential Medium (Biochrom), 5% fetal bovine serum, 5% horse serum, 1% glutamine (2 mM), 0.2% gentamicin (0.1 mg/ml) and glucose (25 mM). Cells were plated onto 20-mm cover slips pre-coated with poly-L-lysine (0.1 mg/ml, Sigma) at a density of 1×10^5 cells/well. Twenty-four hours after plating, the culture medium was replaced with a medium containing: 97.3% Neurobasal medium (Invitrogen), 2% B-27 (Invitrogen), 0.5% glutamine (2 mM), and 0.2% gentamicin (0.1 mg/ml). Finally, after 72 h, the culture medium was replaced with a similar medium lacking glutamine and cells were grown for 4-7 more days prior to experiments.

TUNEL staining- Cortical neurons were treated with A β analogues for 48 h and then stained using a terminal deoxynucleotidyl transferase dUTP nick end labeling (TUNEL) assay kit (APO-BrdU Apoptosis Detection kit, Invitrogen) as described previously [31]. Fluorescent signals were visualized using a Nikon Eclipse E400 microscope (Nikon Instruments Inc., Melville, NY) at $\lambda_{ex} = 480$ nm and $\lambda_{em} = 530$ nm. Images were merged using the bundled software "Picture Frame" (Optronics, Goleta, CA). Images were taken from multiple fields in three independent experiments and the number of TUNEL-positive cells divided by the total number of counted cells was expressed as % apoptotic death (mean \pm SEM).

Patch-clamp recording of calcium currents- According to standard protocols, Ba $^{2+}$ was used as charge carrier rather than Ca $^{2+}$ [32]. Macroscopic Ba $^{2+}$ currents flowing through voltage-gated calcium channels (VGCCs) were recorded by patch-clamp in whole-cell configuration [33] using an Axopatch 200B amplifier (Molecular Devices, Sunnyvale, CA). Stimulation and data acquisition were performed using the Digidata 1200 series interface and pCLAMP 9.2 software (Molecular Devices), as described previously [20, 33]. The external solution contained (in mM): NaCl, 125; BaCl $_2$, 10; MgCl $_2$, 1; HEPES, 10; and tetrodotoxin, 2×10^{-4} to block Na $^{+}$ channels. The pH was adjusted to 7.3 with NaOH. The standard internal solution consisted of (in mM): CsCl, 110; tetraethylammonium chloride, 10; MgCl $_2$, 2; EGTA, 10; glucose, 8; and HEPES, 10. To minimize current run-down during experiments, 4.0 mM ATP magnesium salt, 0.25 mM cAMP sodium salt, and 4.0 mM phosphocreatine disodium salt were added to this solution. The pH was adjusted to 7.3 with CsOH. The cell membrane was depolarized every 6 s (pulse duration, 200 ms) to voltages ranging from -50 to +50 mV from the holding potential of -80 mV. Compensation for capacitive transients and leakage currents was achieved on-line with the clamp-amplifier settings and off-line by subtraction of Cd $^{2+}$ -insensitive currents (200 μ M Cd $^{2+}$). Current density (pA/pF) was calculated by dividing current amplitude by cell membrane capacitance, which was measured with the membrane test feature of the pCLAMP 9.2 software. Cells were treated with 10 μ M of each A β analogue for 12 h prior to experiments. All recordings were made at 23–25°C.

Dendritic spine morphology- Primary hippocampal neurons were used to study the dendritic spine morphology as described previously [34]. Briefly, neurons were treated with 3 μ M of each A β analogue for 72 h. The cells then were fixed with 4% paraformaldehyde and individual neuron were stained with 1,1'-dioctadecyl-3,3,3',3'-tetramethylindocarbocyanine perchlorate (DiI, Sigma) as described previously [34] using a Model 5070 micromanipulator (Eppendorf, Westbury, NY). The DiI-labeled neurons were imaged at 100 \times magnification (oil-immersion objective) using a confocal laser-scanning microscope (Leica, Bannockburn, IL). Images were magnified further using a 3 \times zoom so the morphology of individual spines could be determined and subsequently quantified. The Z-stack images were collected at 0.3- μ m intervals to cover the full depth of the dendritic arbors (20-30 μ m) and compressed into a single JPEG image. The numbers of dendritic spines were counted per 100- μ m length of dendritic branches using ImageJ. The dendritic segments were selected randomly among secondary dendrites from apical branches. At least 50 dendritic segments were used for morphometric analysis. Ten to fifteen individual neurons were analyzed for each experimental group.

Circular dichroism spectroscopy (CD)- Samples were incubated at 25°C with continuous agitation at 200 rpm using an orbital shaker. Spectra were recorded every 2 h during the first 12 h, and then at 24, 48, and 72 h, using a J-810 spectropolarimeter (Jasco, Easton, MD) equipped with a thermostable sample cell at 25°C using 1-mm path-length cuvettes. Spectra were collected from 190–260 nm with 1-s

response time, 50-nm/min scan speed, 0.2-nm resolution and 2-nm bandwidth, and averaged after background subtraction. The data are representative of three independent experiments.

Electron microscopy- Samples were incubated at 25°C with continuous agitation using an orbital shaker at 200 rpm. Eight- μ l aliquots were applied to glow-discharged, carbon-coated Formvar grids (Electron Microscopy Science, Hatfield, PA) for 20 min, fixed with 5 μ l of 2.5% glutaraldehyde (Sigma, St. Louis, MO) for 4 min, and stained with 5 μ l of 1% uranyl acetate (Sigma) for 3 min. The solution was wicked off and the grids were air-dried. The morphology was visualized using a CM120 transmission electron microscope (FEI-Philips, Hillsboro, OR).

Results

Effect of WT and oxidized A β on neuronal viability. To investigate the structure–activity relationship of native and oxidized A β variants and gain insight into the mechanism of toxicity, we used TUNEL staining in rat primary cortical neurons (Fig. 1). The TUNEL assay indicates DNA fragmentation as a measurement of apoptosis [35].

A β 40 was found to cause 14 \pm 1% apoptosis (Fig. 1). A β 40-sulfoxide caused 11.5 \pm 0.7% apoptosis, whereas A β 40-sulfone had a similar effect to WT A β 40, 14.3 \pm 0.6% apoptosis. Overall, the differences observed among the A β 40 analogues were not statistically significant. Under the same conditions, A β 42 caused 20.5 \pm 0.5% apoptosis (Fig. 1). Similar to previously described data, A β 42-sulfoxide was significantly less toxic, causing 13.0 \pm 0.7% apoptosis, i.e., a similar level of toxicity to A β 40, as predicted. Surprisingly, however, A β 42-sulfone showed similar toxicity to WT A β 42, causing 19.7 \pm 0.8% apoptosis. These results were unexpected in view of the oligomer size distribution of A β 42-sulfone, which was similar to A β 42-sulfoxide and distinct from that of WT A β 42 [14]. Similar trends were observed in both cortical and hippocampal neurons using the 3-(4,5-dimethylthiazol-2-yl)-2,5-diphenyltetrazolium bromide (MTT) reduction and lactate dehydrogenase (LDH) release assays (data not shown). Thus, three different assays showed that despite the similar increase in dipole moment upon oxidation of Met³⁵ to sulfoxide or sulfone [14, 21], and despite the fact that oxidation had a similar effect on both the sulfoxide and sulfone forms of A β 42 [14], only the sulfoxide form behaved as we predicted and showed similar toxicity to WT A β 40.

Effect of WT and oxidized A β on macroscopic Ca²⁺ currents. Next, we asked whether the behavior of the oxidized forms of A β correlated with more subtle toxic effects. Disruption of Ca²⁺ homeostasis and excitotoxicity are thought to be important mechanisms by which A β disrupts synaptic activity and eventually lead to neuronal death [36]. Disruption of intracellular Ca²⁺ homeostasis long has been implicated both in normal brain aging and in the pathogenesis of AD. Both conditions are characterized by impairment of the neurons' ability to control Ca²⁺ fluxes and recover from Ca²⁺ loads [37]. To assess the effect on Ca²⁺ currents, we measured A β -induced changes in currents flowing through voltage-gated calcium channels (VGCCs) in primary cortical neurons.

In whole-cell patch-clamp recordings, we measured macroscopic Ba²⁺ currents following treatment with the different A β 40 or A β 42 analogues. Previously, treatment of IMR32 cells with 10 μ M A β 42 for 6–24 h was found to yield maximal increase in depolarization-induced Ca²⁺ influx at 12 h [20]. Therefore, we measured Ba²⁺ currents in the experiments described here at 12 h post treatment.

Both A β 40 and A β 42 caused a significant increase ($p < 0.001$) in total Ba²⁺ current densities in cortical neurons (Fig. 2A, B), similar to the previous results obtained using IMR32 cells [20], suggesting that each of them triggered dysregulation of Ca²⁺ channels. The effect of A β 42 was stronger than that of A β 40 (+69% vs. +55%, respectively) though the difference was not statistically significant. In contrast, treatment of the cells with A β 40- or A β 42-sulfoxide had no effect on total Ba²⁺ currents. In agreement with the measurements of cell viability, the sulfone form of A β 40 and A β 42 caused an increase in Ba²⁺ current densities to the same magnitude as the corresponding WT A β form (Fig. 2A, B). The data suggest that in contrast to the WT and sulfone forms of A β , under the experimental conditions used, the weak toxicity afflicted by A β -sulfoxide was not associated with significant changes in VGCC signals.

Previously, L-type Ca^{2+} (Ca_v1) channels were found to contribute significantly to the current increase induced by A β 42 in IMR32 cells and Ca^{2+} influx through these channels was found responsible for the calcium-mediated activation of pro-apoptotic pathways underlying the stronger neurotoxicity of WT A β 42 relative to A β 42-sulfoxide [20]. To determine whether a similar correlation exists between L-current increases and A β neurotoxicity in cortical neurons, and to what extent it is activated by each of the oxidized forms of A β , we studied the A β -induced modulation of current amplitudes before and after applying 5 μM of the selective L-channel blocker nifedipine. Analysis of the data revealed that peak Ba^{2+} currents flowing through L-channels significantly increased following treatment with WT A β 40 or A β 42 (+80% and +98%, respectively; $p < 0.01$), or their respective sulfone forms (+51% and +80%, respectively; $p < 0.01$; Fig. 3C, D) whereas A β 40- or A β 42-sulfoxide did not produce significant changes.

A β -induced perturbation of dendritic spines. Dendritic spines are semiautonomous compartments containing molecular machinery important for synaptic transmission and plasticity [38]. The number of dendritic spines per unit length of the dendrite in the adult brain is indicative of the number of excitatory synapses present. Examination of postmortem brains from patients with AD or Down syndrome dementia has shown substantial loss of dendritic spines [39].

We analyzed dendritic spines from apical branches of hippocampal pyramidal neurons following treatment with A β 42 or its oxidized analogues (Fig. 3). In initial experiments, we found that 3 μM A β 42 induced a robust effect on dendritic spine number and morphology in this assay, whereas 10 μM led to overt cell death that precluded observation of the effect on dendritic spines. Therefore, we used 3 μM for comparison of WT and oxidized A β 42 analogues. Because the toxicity of A β 40 was substantially lower than that of A β 42 in cell viability assays (Fig. 1 and data not shown for MTT and LDH assays), we did not use A β 40 in this assay.

Following treatment with 3 μM A β 42, the dendrites showed abundant varicosities and the number of dendritic spines per 100 μm decreased to <30% of that in cells treated with medium (Fig. 3B, E). Consistent with the cell viability assays described above, A β 42-sulfoxide showed little induction of varicosities and had a significantly weaker effect on dendritic spine density compared to WT A β 42, decreasing the number of dendritic spines per 100 μm to ~70% of medium-treated cells (Fig. 3C, E). In contrast, and consistent with the other assays results, A β 42-sulfone induced abundant varicosities and decreased the dendritic spine density to the same level as WT A β 42 (Fig. 3D, E).

Assembly kinetics of WT and oxidized A β . Because the biological activity of A β 42-sulfone contradicted our predictions, which were based on the initial oligomer size distributions for the WT and oxidized A β 42 analogues, we asked whether the bioactivity correlated with aggregation kinetics. Early studies of the effect of Met oxidation to sulfoxide on A β assembly have led to mixed results [40, 41], whereas most of the later studies reported that assembly kinetics of A β -sulfoxide was decreased relative to WT A β .

We used CD spectroscopy to study the effect of Met³⁵ oxidation on β -sheet formation during A β fibrillogenesis at the same concentration as used for cell viability measurements (Fig. 4). All the peptides showed an initial CD spectrum characterized by a minimum at 196–200 nm, suggesting that the conformation was predominantly statistical coil. A β 40 showed a gradual decrease in the magnitude of this minimum over 72 h, at which point a maximum at 197–198 nm appeared (Fig. 4A), suggesting an increase in β -sheet content. Observation of the β -sheet-characteristic minimum at 215–218 nm required higher concentration of A β 40 (data not shown). For consistency with other measurements, we kept the concentration at 10 μM in the presented experiments. A β 40-sulfoxide (Fig. 4B) and A β 40-sulfone (Fig. 4C) showed somewhat slower conformational conversion during the first 24 h, though the overall rate of conformational change over 72 h was similar to that of WT A β 40. In both cases, at 48–72 h the spectrum did not show the expected maximum at 197–198 nm and instead appeared nearly flat. However, in each case the solution remained free of particulate material or precipitates suggesting that the spectrum reflected *bona fide* conformational change rather than precipitation of aggregated material.

The spectrum of A β 42 showed a conversion from a minimum at 197 nm to a maximum at 198 nm within 24 h, with concomitant appearance of a minimum at 217–218 nm, indicating conversion from statistical coil to a β -sheet-rich conformation (Fig. 4D). The spectra showed an isodichroic point at 210 nm, suggesting that other conformations did not accumulate to a significant extent. In contrast, the spectrum of A β 42-sulfoxide did not change during the first 24 h of measurement (Fig. 4E), consistent with previous observations of delayed aggregation and β -sheet formation of this peptide relative to WT A β 42 [42]. At later time points (48–72 h), A β 42-sulfoxide did show slow conversion to a typical β -sheet-rich conformation (data not shown). The slow conformational transition of A β 42-sulfoxide correlated with the lack of paranucleus formation by this peptide [14] and with the low toxicity described above. Also in correlation with its biological activity, A β 42-sulfone behaved similarly to WT A β 42. Following a short lag phase, the CD spectrum changed from predominantly statistical coil to β -sheet-rich with an isodichroic point at 210 nm.

To test whether the conformational transition observed by CD spectroscopy correlated with fibril formation, we examined morphological changes in A β 40 and A β 42 in their native, sulfoxide, or sulfone forms by EM (Fig. 5). All the peptides initially had non-fibrillar morphology and showed structures consistent with oligomers. The morphology of A β 40 remained non-fibrillar for 48 h. At 72 h of incubation, typical amyloid fibrils were present together with remaining non-fibrillar structures, and by 96 h, fibrils largely predominated the morphology of A β 40. A β 40-sulfoxide, and A β 40-sulfone both followed similar, albeit slower, morphological changes. Both peptides were still non-fibrillar at 72 h and formed fibrils by 96 h. Thus, fibril formation was delayed by ~24 h relative to WT A β 40. The fibrils of A β 40-sulfoxide were scarce relative to those of WT A β 40 or A β 40-sulfone. These data were consistent with the kinetic trends observed by CD.

As expected, fibril formation by A β 42 analogues was faster than by A β 40 analogues. Correlating with the conformational transition observed by CD and with the toxicity data, A β 42 and A β 42-sulfone had similar kinetics and showed abundant fibrils following 24 h of incubation, whereas A β 42-sulfoxide was non-fibrillar at this time point and showed fibril formation only after 48 h.

The environment the peptides experience in cell culture experiments is different from the hypotonic buffer used in our CD and EM experiments and may affect peptide assembly. Detailed structural investigation of peptide conformation and morphology using CD and EM, respectively, is not possible in the cell culture environment, which includes media, serum, and the cells themselves. However, investigating the structures the cell culture media (without serum or cells) may provide clues to the behavior of the peptides in this environment. Therefore, we incubated the peptides at the same concentration (10 μ M) in DMEM at 37°C and investigated their conformation and morphology periodically for several days. The results are shown in Figs. S1 and S2, supplementary online material.

CD spectra could be obtained in media only down to 203 nm because at lower wavelengths the dynode voltage exceeded the instrument's recommended limits. Thus, the minimum and maximum molar ellipticity at 195–198 that characterize statistical coil and β -strand, respectively, could not be observed. In addition, the noise level was higher than in the spectra obtained in buffer. Nevertheless, temporal changes were observed consistent with conformational transition. Under these conditions, the conformational transition happened in all cases with faster kinetics than in buffer and appeared to be complete or nearly complete by 24 h (Fig. S1). A β 40 (Fig. S1A) and A β 40-sulfone (Fig. S1C) appeared to have similar kinetics of conformational transition, whereas the kinetics of A β 40-sulfoxide was somewhat slower (Fig. 1B). A similar trend was observed for the A β 42 analogues (Fig. S1D–F) though the high noise levels made it difficult to draw unambiguous conclusions.

Consistent with the CD data, all the peptides showed amorphous structure at $t = 0$ h, though not in all cases could those be distinguished from structures observed in the media itself (Fig. S2). All the peptides formed fibrils within 24 h of incubation in media. A β 40 formed abundant short fibrils that were mixed with amorphous structures at 24 and 48 h. At 24 h, the fibrils of A β 40-sulfoxide and A β 40-sulfone appeared longer than those of WT A β 40 and looked ribbon-like, comprising up to 7 protofilaments. Amorphous structures were observed together with the fibrils at this time point in A β 40-

sulfoxide, but not A β 40-sulfone samples. Interestingly, by 48 h, the fibrils of both oxidized forms appeared shorter than at 24 h. A β 42 analogues behaved similarly and were assembled into fibrils by 24 h. At this time point, amorphous aggregates were observed together with fibrils only for A β 42-sulfoxide, but not for WT A β 42 or A β 42-sulfone. The fibrillation process for the latter two peptides appeared to be complete by 24 h.

Discussion

The high toxicity we found for A β 42-sulfone (Figs. 1–3) contradicted our expectations, which were based on the difference between the oligomer size distributions of A β 42-sulfoxide and A β 42-sulfone, and that of WT A β 42 [14], the calculated dipole moments of Met, Met-sulfoxide, and Met-sulfone (Table 1), and structures predicted in several modeling studies [10, 21–23]. Despite the similarity between the behaviors of the sulfoxide and sulfone forms of A β 42, and the difference between the two oxidized forms and WT A β 42, A β 42-sulfone was as toxic as WT A β 42. Several mechanisms may explain these unexpected observations. Here we tested the hypothesis that the toxicity correlated with aggregation rather than with early oligomerization.

The toxicity levels of the WT and oxidized A β 42 analogues correlated with their kinetics of β -sheet and fibril formation (Figs. 4, 5). One interpretation of the data is that the toxic effect may be mediated by later-forming, large oligomers or aggregates rather than by initial small oligomers. Currently, there is no consensus regarding the size and type of A β oligomers that contribute the most to toxicity, or even concerning whether certain oligomers are more important than others for AD pathology. Side-by-side comparison of small and large oligomer populations made of synthetic A β and fractionated from the same initial source has suggested that larger structures were more toxic than small ones [43]. A recent examination of individual A β 40 oligomers stabilized by PICUP has shown a correlation between increased oligomer size and toxicity [44], yet the study found substantial toxicity already for dimers, trimers, and tetramers. Comparison of memory impairment in rats induced by A β oligomers of different sizes from synthetic, cell culture, or transgenic animal brain sources has suggested that small oligomers were more toxic than larger ones [45].

Though high-resolution structures for A β oligomers are beginning to emerge [46], direct structure–activity comparisons among small and large oligomers are difficult. Thus, whether or not the trends we observed among assembly kinetics and toxicity of the different A β analogues represent cause and effect relationship or a mere correlation is an open question. An answer to this question may be provided in future studies by electrophysiologic experiments comparing the sulfoxide and sulfone forms of A β 42 because such experiments can measure toxic effects induced by A β oligomers within minutes, likely before substantial amounts of larger oligomers form [47].

Alternatively, we may explain our findings by questioning our fundamental assumptions. Based on the similarity in the dipole moments of the sulfoxide and sulfone groups (Table 1) and the similarity between the oligomer size distributions of A β 42-sulfoxide and A β 42-sulfone, we assumed that the three-dimensional structure of the oligomers formed by the two oxidized A β 42 analogues was similar (and distinct from that of WT A β 42). We postulated that because of the large increase in dipole moment upon oxidation, the hydrophobic Met side chain, which presumably is shielded from the aqueous solvent in A β 42 oligomers, would partition preferably into the solvent once the sulfide group is oxidized to sulfoxide or sulfone [14]. If such a structural change occurs in A β 42-sulfoxide but not in A β 42-sulfone, it would explain why the sulfone form is as toxic as WT A β 42. This explanation is unlikely and does not account for the similarity in the oligomer size distribution between A β 42-sulfoxide and A β 42-sulfone.

Yet another alternative explanation of the data is that the intrinsic toxicity of the WT, sulfoxide, and sulfone forms of A β are similar and, in the case of A β 42, are unrelated to the oligomer size distributions observed using PICUP, but a cellular response unique to the sulfoxide form reduces its toxicity relative to the WT and sulfone forms. One such cellular response might be an increase in expression levels of methionine-sulfoxide reductase A (MsrA), which was reported recently to increase in cells treated by

A β 42-sulfoxide but not WT A β 42 [48] and may provide a protective effect to the cells. Our data suggest that such protection likely is not entirely responsible for the lower toxicity of A β -sulfoxide because disruption of Ca²⁺ current through VGCC, an important mechanism contributing to A β toxicity, was substantially perturbed by WT A β and A β -sulfone and not at all by A β -sulfoxide. These data suggest that regardless of putative induction of a protective MsrA response, the toxicity of WT A β and A β -sulfone is mediated by at least one mechanism not shared by A β -sulfoxide. Our data also suggest that a substantial portion of A β -sulfoxide remains oxidized and does not get reduced by MsrA during the assay period.

The majority of the studies addressing Met³⁵ oxidation in full-length A β have focused on A β 42 whereas information about A β 40 has been scarce. We found that A β 40 analogues behaved generally similarly to A β 42 analogues, though the differences in toxicity and assembly kinetics were smaller between the WT and oxidized A β 40 peptides. In addition, A β 40-sulfone behaved somewhat more similarly to A β 40-sulfoxide than the counterpart A β 42 analogues. These observations are in line with the lack of change in the oligomer size distribution of WT A β 40 upon oxidation to sulfoxide or sulfone [14] and suggest that in A β 40, the relative contribution of the C-terminal region to the assembly and toxicity behavior is lower than in A β 42, consistent with previous reports [8, 49].

Our study suggests that formation of methionyl radicals and participation of Met in Fenton chemistry [17] likely do not contribute significantly to A β -induced toxicity because A β -sulfone is less likely than A β -sulfoxide to participate in Fenton chemistry or contribute to production of ROS, yet it is as toxic as WT A β . Supporting this view, recently, substitution of Met³⁵ by Val or norleucine (Nle) in A β 40 or A β 42 was reported to yield analogues that were as toxic as the WT peptides [31], though in other experimental systems substitution of Met³⁵ by Nle abolished A β 42 toxicity [15, 20]. Interestingly, a recent study in a transgenic mouse model of AD found that substitution of Met³⁵ by Leu had no effect on learning and memory deficits even though markers of oxidative stress were significantly decreased [50].

In summary, our results suggest a possible correlation between assembly kinetics and toxicity of native and oxidized A β , but demonstrate that the relationships among primary structure, quaternary structure, and toxic activity are complex. Further study will be required to understand why the sulfoxide and sulfone forms of A β 42 have similar electronic characteristics and produce similar oligomer size distributions in PICUP experiments yet behave distinctly in terms of their toxicity and aggregation kinetics.

Acknowledgments

We thank Margaret M. Condon for peptide synthesis and amino acid analysis, Dr. Huiyuan Li for valuable advice and critical discussion of the manuscript, and Dr. David Teplow for the use of his CD spectrometer and plate reader.

Funding

This work was supported by Alzheimer's Association Grant IIRG-07-5833 and NIH/NIA grant AG027818 (G.B.) and by MIUR and UCSC grants (C.G.)

Figure captions

Fig. 1. Native and oxidized A β -induced apoptosis. Rat primary cortical neurons were cultured for 6 d on poly-D-lysine coated cover slips and treated with 10 μ M of each A β analogue for 48 h. The cells then were probed with APO-BrdU for DNA fragmentation. A) Representative micrographs of multiple fields. Red color indicates normal cells. Green-yellow color indicates TUNEL-positive cells. B) The number of apoptotic cells was divided by the total number of cells and expressed as % apoptotic death. The results are mean \pm SEM of three independent experiments. ** $p < 0.01$.

Fig. 2. Effect of native and oxidized A β analogues on calcium currents. Rat primary cortical neurons were treated with 10 μ M of each A β 40 or A β 42 analogue for 12 h. Macroscopic Ba²⁺ currents flowing

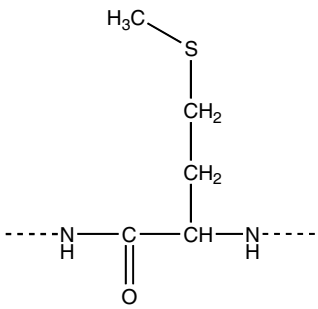
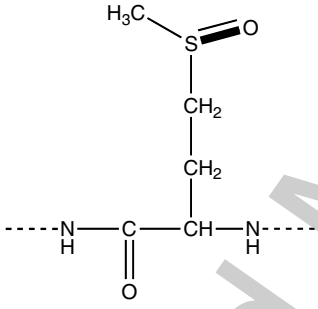
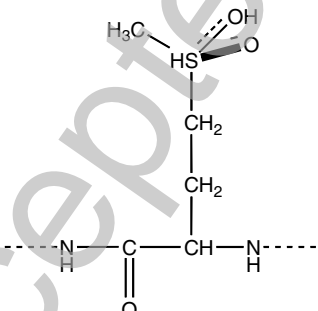
through VGCCs were recorded using patch-clamp in a whole-cell configuration. Current density (pA/pF) was calculated by dividing current amplitude by cell membrane capacitance. A) and B) Current-to-voltage relationships in neurons treated with A β 40 and A β 42 analogues, respectively ($n = 15$ for each group). C) and D) Peak current densities of L-type currents in neurons treated with A β 40 analogues or A β 42 analogues, respectively. $**p < 0.01$.

Fig. 3. Native and oxidized A β 42-induced changes in dendritic spine morphology. Rat primary hippocampal neurons were grown for 21 d, treated with 3 μ M of each A β 42 analogue for 72 h, and stained with DiI. Micrographs are representative of secondary apical branches from multiple neurons. A) Media alone, B) WT A β 42, C) A β 42-sulfoxide, D) A β 42-sulfone. E) Total number of spines in three independent experiments was counted and expressed as mean \pm SEM. $**p < 0.01$.

Fig. 4. Time-dependent conformational transition in native and oxidized A β analogues. Time-dependent conformational changes in A β 40, A β 42, and their respective oxidized analogues were recorded using CD spectroscopy. HFIP-treated peptides were incubated in 10 mM sodium phosphate, pH 7.4. The spectra are representative of at least three independent experiments. A) WT A β 40, B) A β 40-sulfoxide, C) A β 40-sulfone, D) WT A β 42, E) A β 42-sulfoxide, F) A β 42-sulfone.

Fig. 5. Morphology of native and oxidized A β analogues. A β analogues were incubated in sodium phosphate, pH 7.4, and aliquots were spotted on glow-discharged, carbon-coated grids, stained with 1% uranyl acetate, and examined by EM. Each image is representative of three independent experiments.

Table 1. Structure and calculated dipole moments (in Debye) of Met and its oxidized forms.

Residue	Structure	Dipole Moment [14]	Dipole Moment [21]
Met		1.60	1.76
Met-sulfoxide		5.28	3.72
Met-sulfone		5.20	4.30

THIS IS NOT THE VERSION OF RECORD - see doi:10.1042/BJ20101391

References

- 1 Cummings, J. L. (2004) Alzheimer's disease. *N. Engl. J. Med.* **351**, 56-67
- 2 Selkoe, D. J. (2001) Alzheimer's disease: Genes, proteins, and therapy. *Physiol. Rev.* **81**, 741-766
- 3 Kirkitadze, M. D., Bitan, G. and Teplow, D. B. (2002) Paradigm shifts in Alzheimer's disease and other neurodegenerative disorders: The emerging role of oligomeric assemblies. *J. Neurosci. Res.* **69**, 567-577
- 4 Dahlgren, K. N., Manelli, A. M., Stine, W. B., Jr., Baker, L. K., Krafft, G. A. and LaDu, M. J. (2002) Oligomeric and fibrillar species of amyloid- β peptides differentially affect neuronal viability. *J. Biol. Chem.* **277**, 32046-32053
- 5 Scheuner, D., Eckman, C., Jensen, M., Song, X., Citron, M., Suzuki, N., Bird, T. D., Hardy, J., Hutton, M., Kukull, W., Larson, E., Levy-Lahad, E., Viitanen, M., Peskind, E., Poorkaj, P., Schellenberg, G., Tanzi, R., Wasco, W., Lannfelt, L., Selkoe, D. J. and Younkin, S. (1996) Secreted amyloid β -protein similar to that in the senile plaques of Alzheimer's disease is increased *in vivo* by the Presenilin 1 and 2 and APP mutations linked to familial Alzheimer's disease. *Nat. Med.* **2**, 864-870
- 6 Suo, Z. M., Humphrey, J., Kundtz, A., Sethi, F., Placzek, A., Crawford, F. and Mullan, M. (1998) Soluble Alzheimers β -amyloid constricts the cerebral vasculature *in vivo*. *Neurosci. Lett.* **257**, 77-80
- 7 Jarrett, J. T., Berger, E. P. and Lansbury, P. T., Jr. (1993) The C-terminus of the β protein is critical in amyloidogenesis. *Ann. N.Y. Acad. Sci.*, 144-148
- 8 Bitan, G., Kirkitadze, M. D., Lomakin, A., Vollers, S. S., Benedek, G. B. and Teplow, D. B. (2003) Amyloid β -protein ($A\beta$) assembly: $A\beta_{40}$ and $A\beta_{42}$ oligomerize through distinct pathways. *Proc. Natl. Acad. Sci. USA.* **100**, 330-335
- 9 Bernstein, S. L., Dupuis, N. F., Lazo, N. D., Wytenbach, T., Condrón, M. M., Bitan, G., Teplow, D. B., Shea, J.-E., Ruotolo, B. T., Robinson, C. V. and Bowers, M. T. (2009) Amyloid- β protein oligomerization and the importance of tetramers and dodecamers in the aetiology of Alzheimer's disease. *Nat. Chem.* **1**, 326-331
- 10 Urbanc, B., Cruz, L., Yun, S., Buldyrev, S. V., Bitan, G., Teplow, D. B. and Stanley, H. E. (2004) *In silico* study of amyloid β -protein folding and oligomerization. *Proc. Natl. Acad. Sci. USA.* **101**, 17345-17350
- 11 Yan, Y. and Wang, C. (2006) $A\beta_{42}$ is more rigid than $A\beta_{40}$ at the C terminus: implications for $A\beta$ aggregation and toxicity. *J. Mol. Biol.* **364**, 853-862
- 12 Lazo, N. D., Grant, M. A., Condrón, M. C., Rigby, A. C. and Teplow, D. B. (2005) On the nucleation of amyloid β -protein monomer folding. *Protein Sci.* **14**, 1581-1596
- 13 Näslund, J., Schierhorn, A., Hellman, U., Lannfelt, L., Roses, A. D., Tjernberg, L. O., Silberring, J., Gandy, S. E., Winblad, B., Greengard, P. and et al. (1994) Relative abundance of Alzheimer $A\beta$ amyloid peptide variants in Alzheimer disease and normal aging. *Proc. Natl. Acad. Sci. USA.* **91**, 8378-8382
- 14 Bitan, G., Tarus, B., Vollers, S. S., Lashuel, H. A., Condrón, M. M., Straub, J. E. and Teplow, D. B. (2003) A molecular switch in amyloid assembly: Met³⁵ and amyloid β -protein oligomerization. *J. Am. Chem. Soc.* **125**, 15359-15365
- 15 Butterfield, D. A. and Boyd-Kimball, D. (2005) The critical role of methionine 35 in Alzheimer's amyloid β -peptide (1-42)-induced oxidative stress and neurotoxicity. *Biochim. Biophys. Acta.* **1703**, 149-156
- 16 Choi, J., Sullards, M. C., Olzmann, J. A., Rees, H. D., Weintraub, S. T., Bostwick, D. E., Gearing, M., Levey, A. I., Chin, L. S. and Li, L. (2006) Oxidative damage of DJ-1 is linked to sporadic Parkinson and Alzheimer diseases. *J. Biol. Chem.* **281**, 10816-10824

- 17 Ali, F. E., Separovic, F., Barrow, C. J., Cherny, R. A., Fraser, F., Bush, A. I., Masters, C. L. and Barnham, K. J. (2005) Methionine regulates copper/hydrogen peroxide oxidation products of A β . *J. Pept. Sci.* **11**, 353-360
- 18 Palmblad, M., Westlind-Danielsson, A. and Bergquist, J. (2002) Oxidation of methionine 35 attenuates formation of amyloid β -peptide 1-40 oligomers. *J. Biol. Chem.* **277**, 19506-19510
- 19 Hou, L., Shao, H., Zhang, Y., Li, H., Menon, N. K., Neuhaus, E. B., Brewer, J. M., Byeon, I. J., Ray, D. G., Vitek, M. P., Iwashita, T., Makula, R. A., Przybyla, A. B. and Zagorski, M. G. (2004) Solution NMR studies of the A β (1-40) and A β (1-42) peptides establish that the Met35 oxidation state affects the mechanism of amyloid formation. *J. Am. Chem. Soc.* **126**, 1992-2005
- 20 Piacentini, R., Ripoli, C., Leone, L., Misiti, F., Clementi, M. E., D'Ascenzo, M., Giardina, B., Azzena, G. B. and Grassi, C. (2008) Role of methionine 35 in the intracellular Ca²⁺ homeostasis dysregulation and Ca²⁺-dependent apoptosis induced by amyloid β -peptide in human neuroblastoma IMR32 cells. *J. Neurochem.* **107**, 1070-1082
- 21 Triguero, L., Singh, R. and Prabhakar, R. (2008) Comparative molecular dynamics studies of wild-type and oxidized forms of full-length Alzheimer amyloid β -peptides A β (1-40) and A β (1-42). *J. Phys. Chem. B.* **112**, 7123-7131
- 22 Yang, M. and Teplow, D. B. (2008) Amyloid β -protein monomer folding: free-energy surfaces reveal alloform-specific differences. *J. Mol. Biol.* **384**, 450-464
- 23 Urbanc, B., Betnel, M., Cruz, L., Bitan, G. and Teplow, D. B. (2010) Elucidation of amyloid β -protein oligomerization mechanisms: discrete molecular dynamics study. *J. Am. Chem. Soc.* **132**, 4266-4280
- 24 Varadarajan, S., Kanski, J., Aksenova, M., Lauderback, C. and Butterfield, D. A. (2001) Different mechanisms of oxidative stress and neurotoxicity for Alzheimer's A β (1-42) and A β (25-35). *J. Am. Chem. Soc.* **123**, 5625-5631
- 25 Moskovitz, J. (2005) Methionine sulfoxide reductases: ubiquitous enzymes involved in antioxidant defense, protein regulation, and prevention of aging-associated diseases. *Biochim. Biophys. Acta.* **1703**, 213-219
- 26 Binger, K. J., Griffin, M. D., Heinemann, S. H. and Howlett, G. J. (2010) Methionine-oxidized amyloid fibrils are poor substrates for human methionine sulfoxide reductases A and B2. *Biochemistry.* **49**, 2981-2983
- 27 Ejiri, S. I., Weissbach, H. and Brot, N. (1979) Reduction of methionine sulfoxide to methionine by *Escherichia coli*. *J. Bacteriol.* **139**, 161-164
- 28 Rahimi, F., Maiti, P. and Bitan, G. (2009) Photo-induced cross-linking of unmodified proteins (PICUP) applied to amyloidogenic peptides. *J. Vis. Exp.* **23**, <http://www.jove.com/index/details.stp?id=1071>
- 29 Segal, M. and Manor, D. (1992) Confocal microscopic imaging of [Ca²⁺]_i in cultured rat hippocampal neurons following exposure to *N*-methyl-D-aspartate. *J. Physiol.* **448**, 655-676
- 30 Dravid, S. M. and Murray, T. F. (2004) Spontaneous synchronized calcium oscillations in neocortical neurons in the presence of physiological [Mg(2+)]: involvement of AMPA/kainate and metabotropic glutamate receptors. *Brain Res.* **1006**, 8-17
- 31 Maiti, P., Lomakin, A., Benedek, G. B. and Bitan, G. (2010) Despite its role in assembly, methionine 35 is not necessary for amyloid β -protein toxicity. *J. Neurochem.* **113**, 1252-1262
- 32 Hamill, O. P., Marty, A., Neher, E., Sakmann, B. and Sigworth, F. J. (1981) Improved patch-clamp techniques for high-resolution current recording from cells and cell-free membrane patches. *Pflugers Arch.* **391**, 85-100
- 33 Piacentini, R., Ripoli, C., Mezzogori, D., Azzena, G. B. and Grassi, C. (2008) Extremely low-frequency electromagnetic fields promote in vitro neurogenesis via upregulation of Ca_v1-channel activity. *J. Cell. Physiol.* **215**, 129-139
- 34 Papa, M., Bundman, M. C., Greenberger, V. and Segal, M. (1995) Morphological analysis of dendritic spine development in primary cultures of hippocampal neurons. *J. Neurosci.* **15**, 1-11

- 35 Smale, G., Nichols, N. R., Brady, D. R., Finch, C. E. and Horton, W. E., Jr. (1995) Evidence for apoptotic cell death in Alzheimer's disease. *Exp. Neurol.* **133**, 225-230
- 36 Barger, S. W. (2004) An unconventional hypothesis of oxidation in Alzheimer's disease: intersections with excitotoxicity. *Front. Biosci.* **9**, 3286-3295
- 37 Thibault, O., Gant, J. C. and Landfield, P. W. (2007) Expansion of the calcium hypothesis of brain aging and Alzheimer's disease: minding the store. *Aging Cell.* **6**, 307-317
- 38 Nimchinsky, E. A., Sabatini, B. L. and Svoboda, K. (2002) Structure and function of dendritic spines. *Annu. Rev. Physiol.* **64**, 313-353
- 39 Takashima, S., Ieshima, A., Nakamura, H. and Becker, L. E. (1989) Dendrites, dementia and the Down syndrome. *Brain Dev.* **11**, 131-133
- 40 Snyder, S. W., Lador, U. S., Wade, W. S., Wang, G. T., Barrett, L. W., Matayoshi, E. D., Huffaker, H. J., Krafft, G. A. and Holzman, T. F. (1994) Amyloid- β aggregation: selective inhibition of aggregation in mixtures of amyloid with different chain lengths. *Biophys. J.* **67**, 1216-1228
- 41 Watson, A. A., Fairlie, D. P. and Craik, D. J. (1998) Solution structure of methionine-oxidized amyloid β -peptide (1-40) - Does oxidation affect conformational switching? *Biochemistry.* **37**, 12700-12706
- 42 Hou, L., Kang, I., Marchant, R. E. and Zagorski, M. G. (2002) Methionine 35 oxidation reduces fibril assembly of the amyloid β -(1-42) peptide of Alzheimer's disease. *J. Biol. Chem.* **277**, 40173-40176.
- 43 Hepler, R. W., Grimm, K. M., Nahas, D. D., Breese, R., Dodson, E. C., Acton, P., Keller, P. M., Yeager, M., Wang, H., Shughrue, P., Kinney, G. and Joyce, J. G. (2006) Solution state characterization of amyloid β -derived diffusible ligands. *Biochemistry.* **45**, 15157-15167
- 44 Ono, K., Condon, M. M. and Teplow, D. B. (2009) Structure-neurotoxicity relationships of amyloid β -protein oligomers. *Proc. Natl. Acad. Sci. USA.* **106**, 14745-14750
- 45 Reed, M. N., Hofmeister, J. J., Jungbauer, L., Welzel, A. T., Yu, C., Sherman, M. A., Lesne, S., Ladu, M. J., Walsh, D. M., Ashe, K. H. and Cleary, J. P. (2009) Cognitive effects of cell-derived and synthetically derived A β oligomers. *Neurobiol. Aging*
- 46 Yu, L., Edalji, R., Harlan, J. E., Holzman, T. F., Lopez, A. P., Labkovsky, B., Hillen, H., Barghorn, S., Ebert, U., Richardson, P. L., Miesbauer, L., Solomon, L., Bartley, D., Walter, K., Johnson, R. W., Hajduk, P. J. and Olejniczak, E. T. (2009) Structural characterization of a soluble amyloid β -peptide oligomer. *Biochemistry.* **48**, 1870-1877
- 47 Fradinger, E. A., Monien, B. H., Urbanc, B., Lomakin, A., Tan, M., Li, H., Spring, S. M., Condon, M. M., Cruz, L., Xie, C. W., Benedek, G. B. and Bitan, G. (2008) C-terminal peptides coassemble into A β 42 oligomers and protect neurons against A β 42-induced neurotoxicity. *Proc. Natl. Acad. Sci. USA.* **105**, 14175-14180
- 48 Misiti, F., Clementi, M. E. and Giardina, B. (2010) Oxidation of methionine 35 reduces toxicity of the amyloid β -peptide(1-42) in neuroblastoma cells (IMR-32) via enzyme methionine sulfoxide reductase A expression and function. *Neurochem. Int.* **56**, 597-602
- 49 Bitan, G., Vollers, S. S. and Teplow, D. B. (2003) Elucidation of Primary Structure Elements Controlling Early Amyloid β -Protein Oligomerization. *J. Biol. Chem.* **278**, 34882-34889
- 50 Butterfield, D. A., Galvan, V., Lange, M. B., Tang, H., Sowell, R. A., Spilman, P., Fombonne, J., Gorostiza, O., Zhang, J., Sultana, R. and Bredesen, D. E. (2009) In vivo oxidative stress in brain of Alzheimer disease transgenic mice: Requirement for methionine 35 in amyloid β -peptide of APP. *Free Radic. Biol. Med.* **48**, 136-144

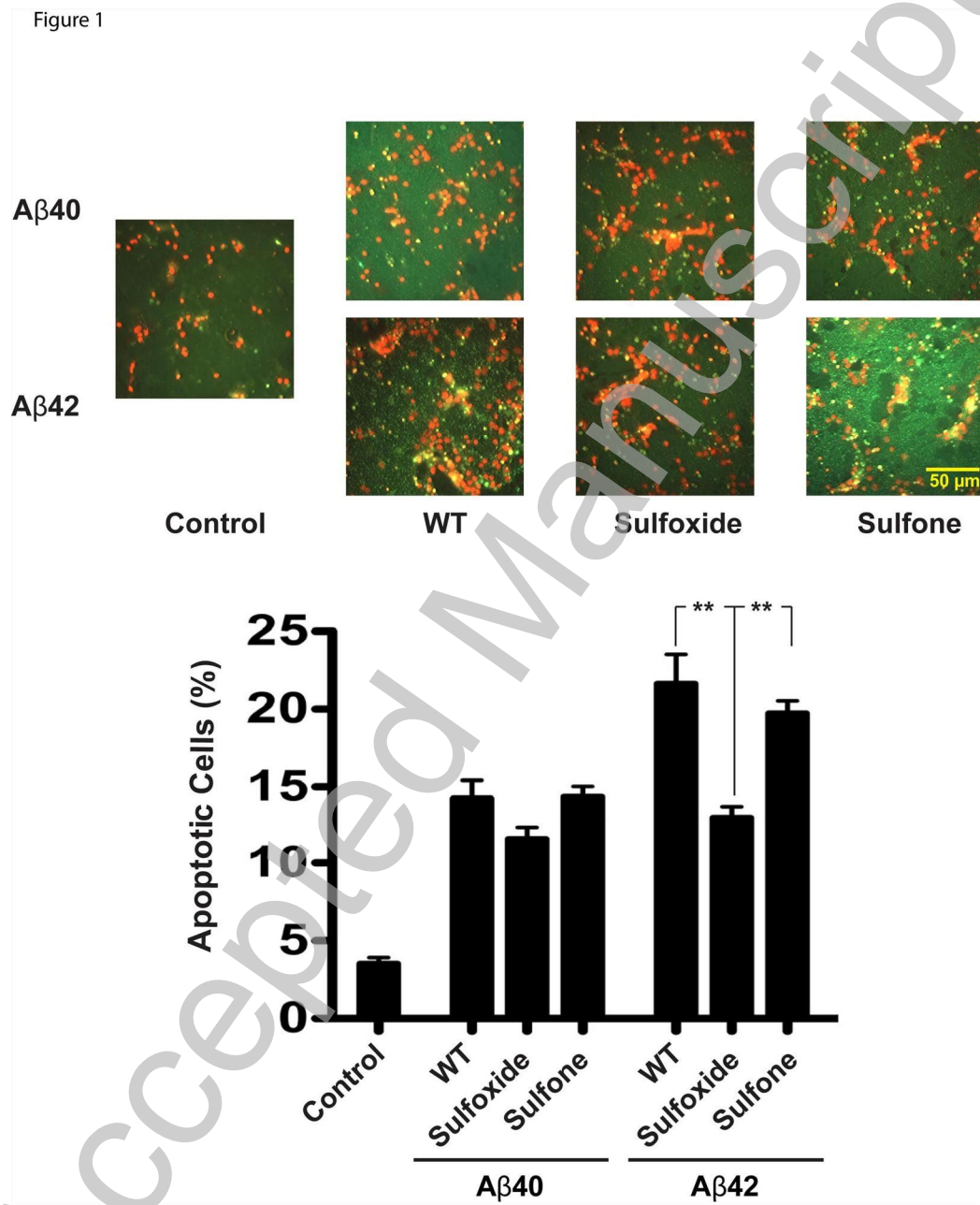
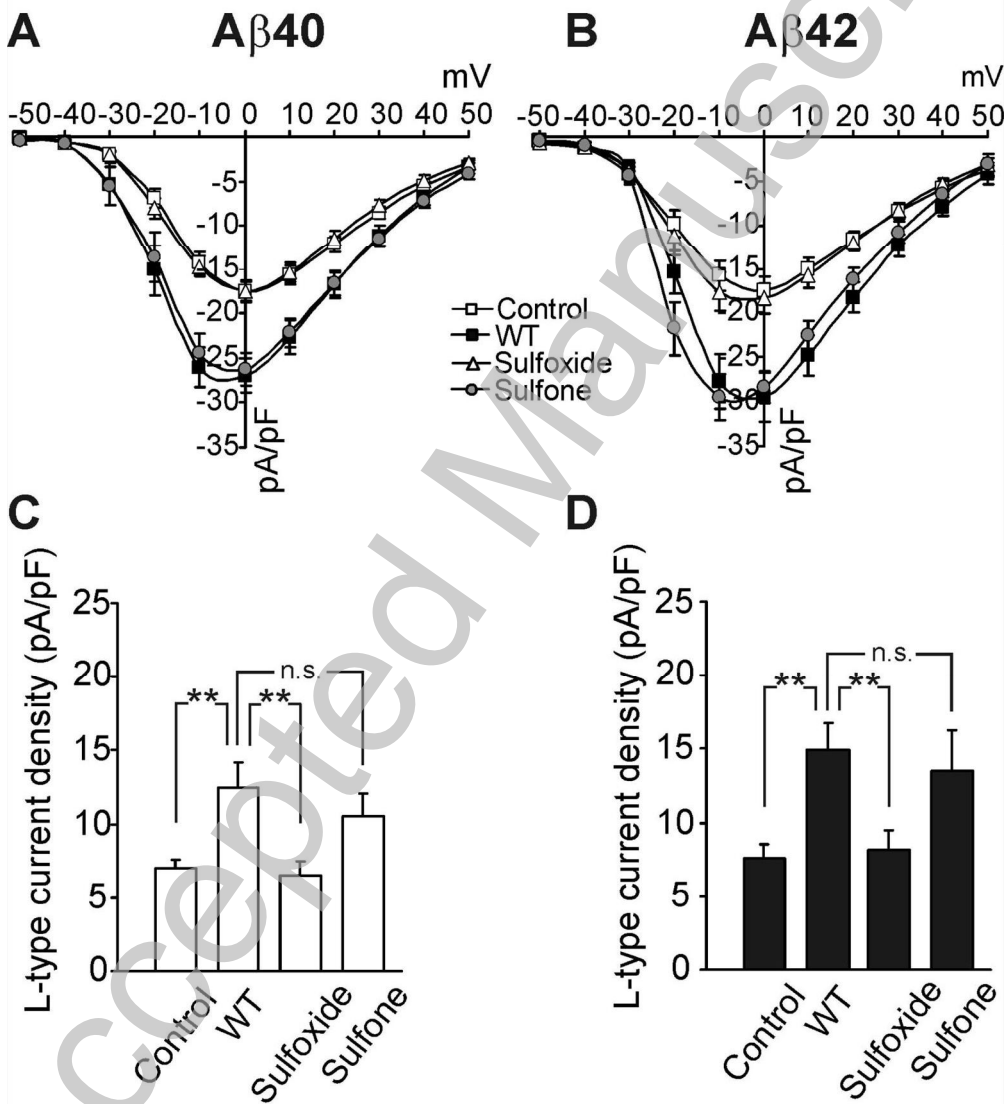


Figure 2



THIS IS NOT THE VERSION OF RECORD - see doi:10.1042/BJ20101391

Figure 3

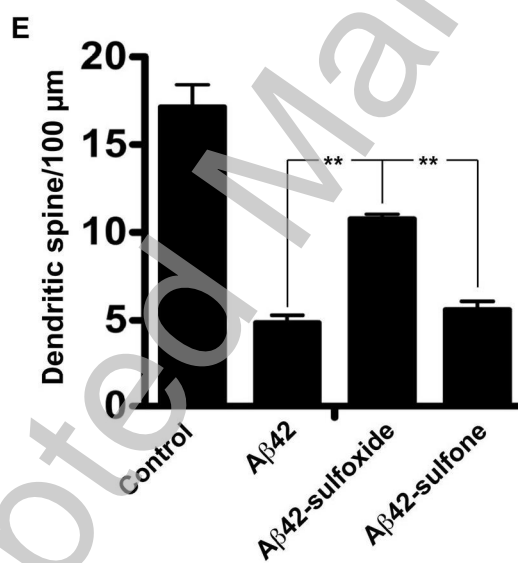
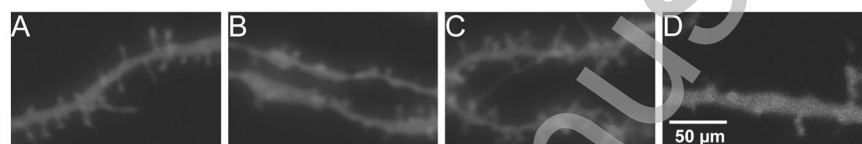
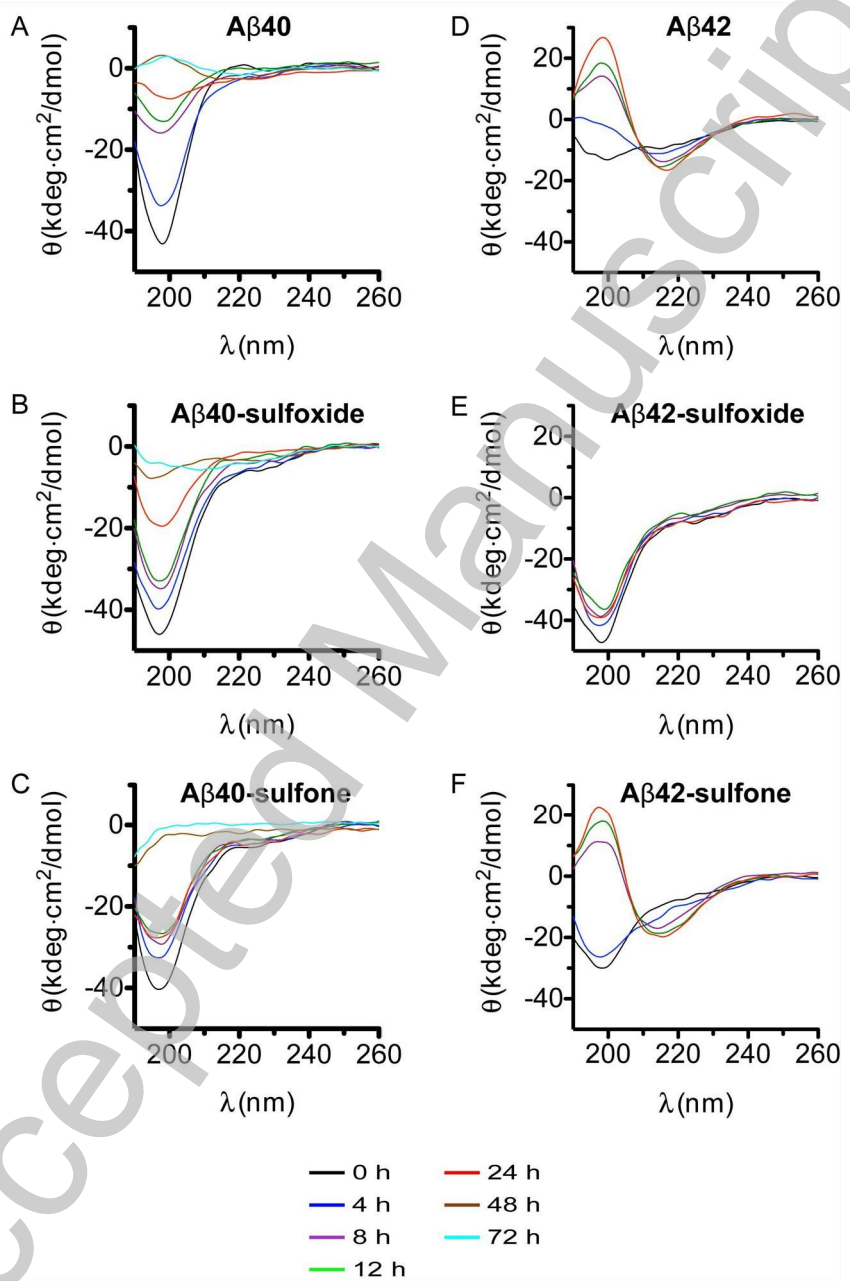


Figure 4



THIS IS NOT THE VERSION OF RECORD - see doi:10.1042/BJ20101391

Accepted Manuscript

Figure 5

